22

Optical Satellite Volcano Monitoring: A Multi-Sensor Rapid Response System

Kenneth A. Duda[1], Michael Ramsey[2], Rick Wessels[3] and Jonathan Dehn[4]
[1]SGT, contractor to U.S. Geological Survey (USGS) Earth Resources Observation and Science (EROS) Center, Sioux Falls, South Dakota; work performed under USGS contract 08HQCN0005. [2]Department of Geology & Planetary Science, University of Pittsburgh, and Advanced Spaceborne Thermal Emission and Reflection Radiometer (ASTER) Science Team.[3]USGS Alaska Volcano Observatory. [4]University of Alaska Fairbanks and Alaska Volcano Observatory. United States of America.

1. Introduction

In this chapter, the use of satellite remote sensing to monitor active geological processes is described. Specifically, threats posed by volcanic eruptions are briefly outlined, and essential monitoring requirements are discussed. As an application example, a collaborative, multi-agency operational volcano monitoring system in the north Pacific is highlighted with a focus on the 2007 eruption of Kliuchevskoi volcano, Russia. The data from this system have been used since 2004 to detect the onset of volcanic activity, support the emergency response to large eruptions, and assess the volcanic products produced following the eruption. The overall utility of such integrative assessments is also summarized.

The work described in this chapter was originally funded through two National Aeronautics and Space Administration (NASA) Earth System Science research grants that focused on the Advanced Spaceborne Thermal Emission and Reflection Radiometer (ASTER) instrument. A skilled team of volcanologists, geologists, satellite tasking experts, satellite ground system experts, system engineers and software developers collaborated to accomplish the objectives. The first project, *Automation of the ASTER Emergency Data Acquisition Protocol for Scientific Analysis, Disaster Monitoring, and Preparedness*, established the original collaborative research and monitoring program between the University of Pittsburgh (UP), the Alaska Volcano Observatory (AVO), the NASA Land Processes Distributed Active Archive Center (LP DAAC) at the U.S. Geological Survey (USGS) Earth Resources Observation and Science (EROS) Center, and affiliates on the ASTER Science Team at the Jet Propulsion Laboratory (JPL) as well as associates at the Earth Remote Sensing Data Analysis Center (ERSDAC) in Japan. This grant, completed in 2008, also allowed for detailed volcanic analyses and data validation during three separate summer field campaigns to Kamchatka Russia. The second project, *Expansion and synergistic use of the ASTER Urgent Request Protocol (URP) for natural disaster monitoring and scientific analysis*, has expanded the project to other volcanoes around the world and is in progress through 2011.

The focus on ASTER data is due to the suitability of the sensor for natural disaster monitoring and the availability of data. The instrument has several unique facets that make it especially attractive for volcanic observations (Ramsey and Dehn, 2004). Specifically, ASTER routinely collects data at night, it has the ability to generate digital elevation models using stereo imaging, it can collect data in various gain states to minimize data saturation, it has a cross-track pointing capability for faster targeting, and it collects data up to ±85° latitude for better global coverage. As with any optical imaging-based remote sensing, the viewing conditions can negatively impact the data quality. This impact varies across the optical and thermal infrared wavelengths as well as being a function of the specific atmospheric window within a given wavelength region. Water vapor and cloud formation can obscure surface data in the visible and near infrared (VNIR)/shortwave infrared (SWIR) region due mainly to non-selective scattering of the incident photons. In the longer wavelengths of the thermal infrared (TIR), scattering is less of an issue, but heavy cloud cover can still obscure the ground due to atmospheric absorption. Thin clouds can be optically-transparent in the VNIR and TIR regions, but can cause errors in the extracted surface reflectance or derived surface temperatures. In regions prone to heavy cloud cover, optical remote sensing can be improved through increased temporal resolution. As more images are acquired in a given time period the chances of a clear image improve dramatically. The Advanced Very High Resolution Radiometer (AVHRR) routine monitoring, which commonly collects 4-6 images per day of any north Pacific volcano, takes advantage of this fact. The rapid response program described in this chapter also improves the temporal resolution of the ASTER instrument.

ASTER has been acquiring images of volcanic eruptions since soon after its launch in December 1999. An early example included the observations of the large pyroclastic flow deposit emplaced at Bezymianny volcano in Kamchatka, Russia. The first images in March 2000, just weeks after the eruption, revealed the extent, composition, and cooling history of this large deposit and of the active lava dome (Ramsey and Dehn, 2004). The initial results from these early datasets spurred interest in using ASTER data for expanded volcano monitoring in the north Pacific. It also gave rise to the multi-year NASA-funded programs of rapid response scheduling and imaging throughout the Aleutian, Kamchatka and Kurile arcs. Since the formal establishment of the programs, the data have provided detailed descriptions of the eruptions of Augustine, Bezymianny, Kliuchevskoi and Sheveluch volcanoes over the past nine years (Wessels et al., in press; Carter et al., 2007, 2008; Ramsey et al., 2008; Rose and Ramsey, 2009).

The initial research focus of this rapid response program was specifically on automating the ASTER sensor's ability for targeted observational scheduling using the expedited data system. This urgent request protocol is one of the unique characteristics of ASTER. It provides a limited number of emergency observations, typically at a much-improved temporal resolution and quicker turnaround with data processing in the United States rather than in Japan. This can speed the reception of the processed data by several days to a week. The ongoing multi-agency research and operational collaboration has been highly successful. AVO serves as the primary source for status information on volcanic activity, working closely with the National Weather Service (NWS), Federal Aviation Administration (FAA), military and other state and federal emergency services. Collaboration with the

Russian Institute of Volcanology and Seismology (IVS)/Kamchatka Volcanic Eruption Response Team (KVERT) is also maintained. Once a volcano is identified as having increased thermal output, ASTER is automatically tasked and the volcano is targeted at the next available opportunity. After the data are acquired, scientists at all the agencies have access to the images, with the primary science analysis carried out at the University of Pittsburgh and AVO. Results are disseminated to the responsible monitoring agencies and the global community through e-mail mailing lists.

2. Overview

Few natural hazards have the devastating impact of large volcanic eruptions (Figure 1). These events can affect scales from the local citizen to the rare global impact where large Plinian eruptions can alter global climate for years to decades (Yang and Schlesinger, 2002). Eruptions can present significant and varying levels of threat to public safety and health by way of explosive forces that launch rocks and ash, destructive pyroclastic lava flows and gaseous emissions, disruption of transportation and communication, introduction of disease and the loss of life. In addition to threats on the ground, aircraft and passengers are at considerable risk if travelling in affected areas (Miller and Casadevall, 2000). This is a particular concern in the north Pacific where numerous flight routes pass over active volcanoes (Figure 2).

Fig. 1. An ash-rich volcanic cloud from the 1989-1990 eruption of Redoubt volcano (courtesy J. Warren, April 21, 1990). Large eruption clouds such as these are a major hazard to commercial aviation in the busy north Pacific corridor.

Therefore, advance warning of incipient volcanic activity can lead to better and more accurate eruption prediction and help to save lives. High-quality and detailed data are needed in order to assess the relative risks posed by any one of the potentially active volcanoes along the Aleutian-Kamchatka-Kurile arcs. These data can include seismic

monitoring, deformational analysis, studies of the emitted gas, visual and thermal observations, as well as the use of orbital remote sensing. The volcanoes can be monitored using in situ equipment, airborne and satellite imaging systems, or some combination of all of these.

Ground-based seismic and deformation measurements commonly provide the earliest indications of renewed activity and subsurface magma movement at a particular volcano (Stephens and Chouet, 2001; Fournier et al., 2009; Lu et al., 2007). Increased seismic activity and a determination of the frequency, depth, and type of earthquakes below a volcano can be leading indicators of later eruptions. Field- or space-based measurements of volcanically induced deformation together with increased levels of heat and gas emissions can further verify the seismic results and lead to a more complete picture of the changes with time. Changes in the alignment of surface features are noted through precise measurements and the collection of spectral, thermal, and GPS data can serve to validate the satellite-based observations.

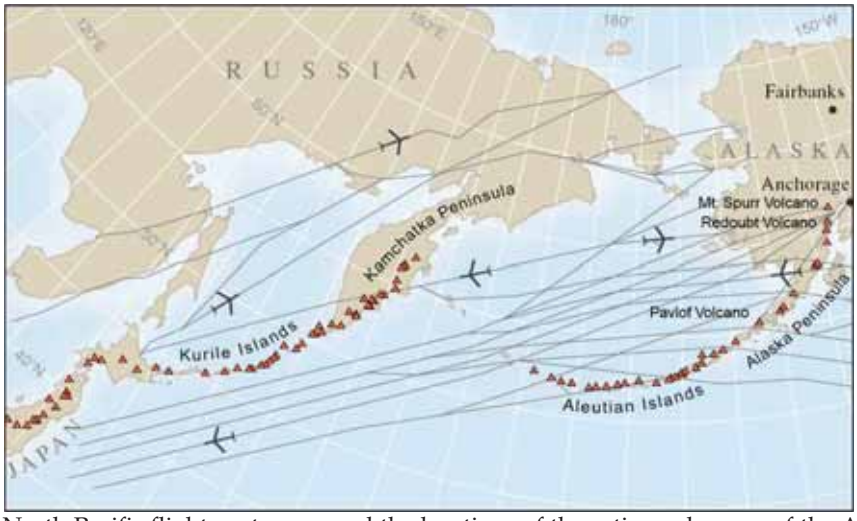

Fig. 2. North Pacific flight route map and the locations of the active volcanoes of the Alaska Peninsula, the Aleutian Islands, the Kamchatka Peninsula, the Kurile Islands, and into Japan (Courtesy USGS Fact Sheet 030-97).

In addition to ground-based measurements, satellite-based observations of volcanoes are of value. Satellite-based observations are useful in the northern Pacific and at many other active volcanoes around the world, where limited resources do not allow extensive ground-based monitoring. Large regions of the world and widely distributed and commonly remote targets can be monitored frequently and economically using satellite data. These images can reveal changes in thermal or gas emission, in the composition of the surface rocks, and in the deformation over time. They can thus provide additional insight into the evolving status of volcanoes. Fixed-wing aircraft and helicopters can also be used where resources permit to carry sensors such as thermal cameras, gas sensors, and cameras, which obtain higher

resolution data of the volcanic activity. The integrated analysis of all available data offers an enhanced perspective on the subtle and unique differences among volcanoes and on the likelihood of impending eruptive activity at a given site.

The scientists and engineers assembled to carry out the previously described NASA-funded research programs have the goal of improving volcanic monitoring in the north Pacific region in order to minimize the subsequent risks and increase scientific knowledge of these dynamic geologic processes. Incorporating the finer spatial resolution, multispectral ASTER data in the analysis process allowed this possibility and added greater clarity to the characterization of many remote volcanoes in the north Pacific region.

The work involved developing and implementing algorithms and tools to detect new activity, establish protocols for escalating response activity, create system linkages between AVO, the LP DAAC and JPL to enable semi-automated transmission of satellite tasking requests, develop the tools and procedures to identify ASTER overpass opportunities and control scheduling requests, secure sensor tasking authorization from the ASTER Science Team, employ existing systems to capture, downlink and process ASTER data, and finally create new data distribution mechanisms to ensure the timely availability of the acquired data. New data analysis procedures are then employed to assess current conditions and issue alerts when needed.

3. Sensors

The critical imaging requirements (i.e., optimum temporal frequency, spatial resolution, wavelengths, etc.) must be understood in order to use sensors on Earth-orbiting spacecraft to monitor volcanoes. The most commonly used instruments for volcano monitoring in the north Pacific include AVHRR, Geostationary Operational Environmental Satellite (GOES), Multifunctional Transport Satellites (MTSAT-1R), Moderate Resolution Imaging Spectroradiometer (MODIS), the Landsat Enhanced Thematic Mapper Plus (ETM+), and ASTER (Table 1). Sub-meter visible data from several commercial satellites (e.g. QuickBird, WorldView, IKONOS and GeoEye) have also recently become integrated as another useful tool for volcano monitoring.

Current sensors such as AVHRR, MODIS, MTSAT, and GOES provide the frequency necessary to detect the onset of large thermal anomalies in near real-time (Dehn et al, 2000; Wright et al., 2002, Schneider et al., 2000). In comparison, high spatial resolution instruments such as ASTER and Landsat ETM+ provide data at a much improved spatial scale ideal for scientific analysis, damage assessment, and smaller scale monitoring, but at the expense of rapid repeat times (Harris et al., 1998; Ramsey and Dehn, 2004). In order to obtain frequent status updates where attempting to initially identify thermal anomalies, sensors offering quick revisits (i.e., GOES, AVHRR, MODIS) are used (Figure 3). The disadvantage is that such data are collected at a coarse spatial resolution allowing only very large or very hot anomalies to be detected, whereas the non-eruptive or small-scale activity is missed completely at many of the remote volcanoes. Higher spatial resolution data (i.e., ASTER, ETM+) are employed in order to obtain more detailed information of lava flows, thermal anomalies, and gas emissions. However, nominally ASTER can only revisit a site once every

16 days at the equator viewing nadir. This temporal frequency is improved with off-nadir pointing and/or at higher latitudes. For example, at the higher latitudes of Kamchatka the temporal frequency can be shortened to 13 hours with off nadir pointing.

The ASTER URP has been used in support of North Pacific volcano monitoring to improve the collection probability and the speed of ASTER data availability. Through this approach, data are typically available within six hours after acquisition. This combination of frequent coarse spatial resolution change detection and less frequent detailed higher resolution imaging has proven very valuable scientifically and operationally. The three bands of ASTER VNIR data span from 0.52 to 0.86 micrometers at a ground resolution of 15 m. These data have been used to generate digital elevation models, map the eruption deposits and changing surface characteristics and to detect ground temperatures in excess of 800 °C. Thermal anomaly and gas emissions identification is accomplished primarily using sensor bands in the SWIR and TIR wavelengths. The six ASTER SWIR bands cover wavelengths from 1.6 to 2.43 micrometers at 30-m ground resolution. Unfortunately, the ASTER SWIR subsystem is no longer operational after 2008, but the data were commonly used to detect alteration minerals on the surface and temperatures between 100 °C and 460 °C. The ASTER TIR subsystem has five TIR bands from 8.125 to 11.65 micrometers at 90-m ground resolution. These data have been used to extract temperatures less than 100 °C, map silicate and carbonate minerals, model the vesicle content of lavas, and estimate the thermal inertia of the surfaces. A brief history of the ASTER mission, including key orbital and data characteristics, is provided in the text box entitled The ASTER Mission.

Criteria	**GOES / MTSAT**	**AVHRR**	**MODIS**	**LANDSAT ETM+**	**ASTER**
Revisit frequency	Geostationary	2 passes per day	1-2 days	16 days	16 days, less off-nadir
Ground resolution	At 60°N latitude: 2 km VIS 8 km IR	1.1 km (LAC)	250m (B1-2), 500m (B3-7), 1000m (B8-36)	30m (B1-5, 7) 60m (B6) 15m (B8)	15m (B1-3), 30m (B4-9), 90m (B10-14)
Spectral coverage	5 bands: 0.55 to 12.5 μm	6 bands: 0.58 to 12.4 μm	36 bands: 0.405 to 14.385 μm	8 bands: 0.45 to 12.5 μm	14 bands: 0.52 to 11.65 μm
Swath Width	Full Earth view	2,399 km	2,330 km	185 km	60 km
Orbit Altitude	35,800 km	833 km	705 km	705 km	705 km

Table 1. Comparison of key characteristics for sensors used in the operational north Pacific monitoring system.

4. Ground Systems and Data Acquisition

The infrastructure needed to support ASTER urgent request tasking, data collection, processing and eventual distribution is summarized in Figure 4. The five key steps of the volcano monitoring sequence are shown in the center of the figure. Corresponding contributions by participating groups are shown in the outer circle, occurring in a sequence that commences at the arrow and proceeds clockwise. The existing ASTER mission procedures and systems were used for final tasking, collection, and data processing.

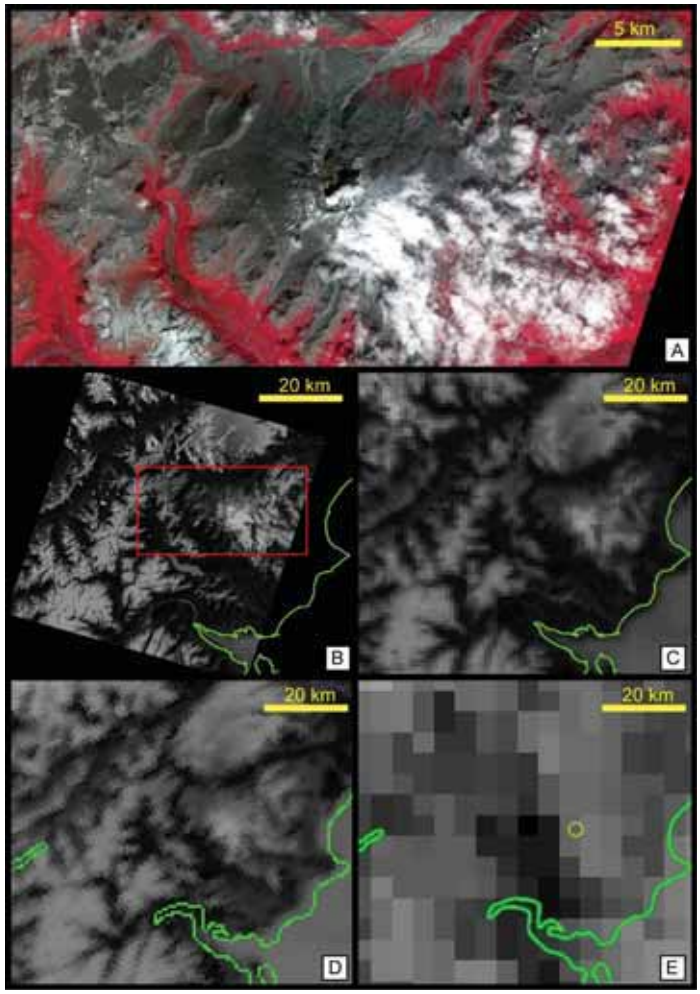

Fig. 3. Comparison of satellite data at several spatial resolutions over Redoubt volcano, Alaska during daylight hours between 21:30 and 22:01 UTC on June 6, 2009. **(A)** False-color subset of ASTER 15 m VNIR bands 3,2,1 as R,G,B. Figures B-E show TIR bands (centered on about 11 micrometers) from four different sensors: **(B)** ASTER 90 m TIR band 14, **(C)** MODIS 1 km TIR band 31, **(D)** AVHRR 1.1km TIR band 4, and **(E)** GOES 8 km TIR band 4.

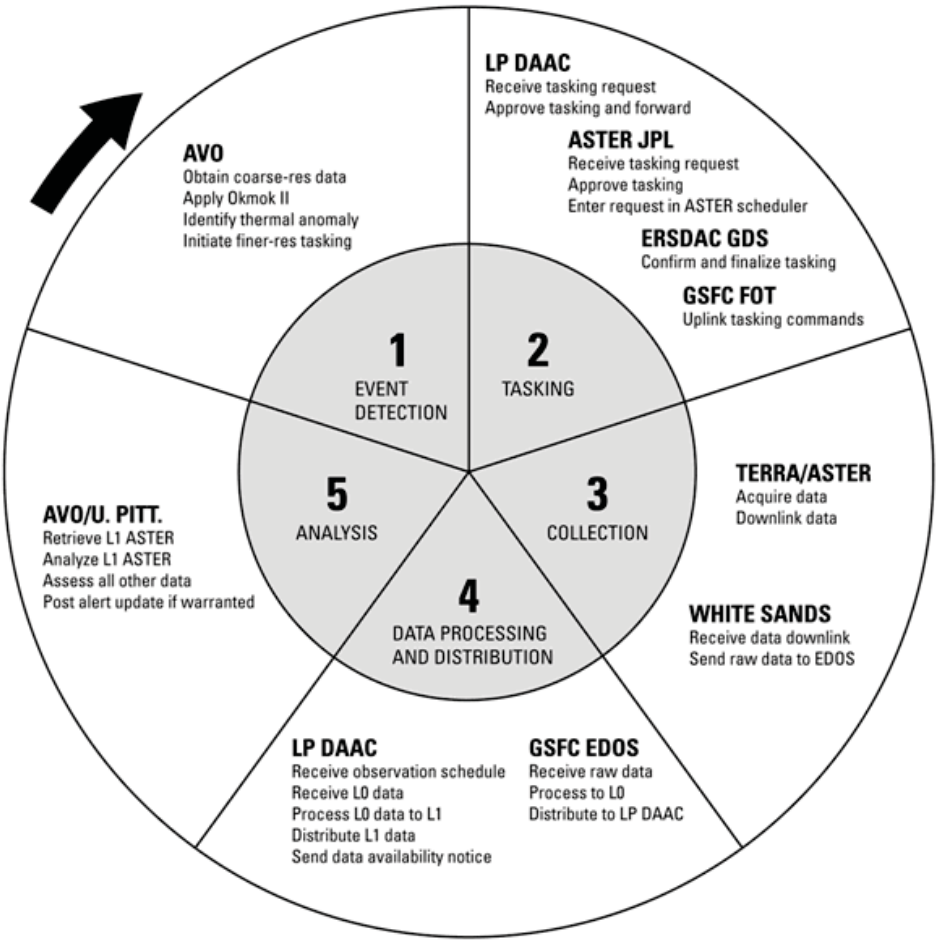

Fig. 4. Volcano monitoring actions and participant involvement. Size of each portion is not scaled to the actual work level involved. Acronyms: Alaska Volcano Observatory (AVO); Advanced Spaceborne Thermal Emission and Reflection Radiometer (ASTER); Jet Propulsion Laboratory (JPL); Earth Remote Sensing Data Analysis Center (ERSDAC); Ground Data System (GDS); Goddard Space Flight Center (GSFC); Flight Operations Team (FOT); Earth Observing System Data and Information System (EOSDIS) Data and Operations System (EDOS); Land Processes Distributed Active Archive Center (LP DAAC); University of Pittsburgh (U. Pitt).

Initial thermal anomaly event detection in AVHRR or MODIS data triggers the ASTER ground systems, scheduling, and eventual data acquisition. The methods used to detect anomalous events include a detailed set of screening algorithms designed to minimize false positives prior to tasking ASTER. Once ASTER is tasked, a series of procedures are used to determine timing, scheduling support, and the eventual distribution of ASTER data. This

entire system of cross-satellite integration and supporting systems is located at AVO; LP DAAC; JPL; ERSDAC; Goddard Space Flight Center (GSFC); White Sands, New Mexico; and includes the ASTER instrument on the Terra spacecraft. The work of this project has contributed new techniques in event detection and tasking of a complex instrument.

4.1 Event Detection

The core of the triggering mechanism for the ASTER emergency acquisition requests is based on the Okmok algorithm (Dean et al., 1998). This algorithm uses a time series of AVHRR data to detect thermal anomalies above an expected average seasonal background temperature. Deviations in temperature may signal increased thermal emission and an impending eruption at a particular volcano. The algorithm scanned a small subsector of data over each volcano for the warmest IR band 3 (3.5-3.9 micrometers) radiant temperature. This value along with all other values in the data subset are recorded and tested based on a simple criterion: if the AVHRR band 3 temperature was greater than 35 °C, then an e-mail was generated and sent to all AVO staff. This process worked well, however its overall effectiveness was limited due to the poor geolocation accuracy of the AVHRR instrument and the generation of numerous false alarms due to noise.

In conjunction with the NASA funded projects, the Okmok algorithm has been significantly refined and applied to other sensors, such as MODIS. It has also been revised to better constrain the AVHRR data stream. The new algorithm, called Okmok II, focuses on decreasing the number of false alarms through a series of additional logic tests (Dehn and Harris, in press). However, it does not sacrifice the sensitivity to low grade thermal anomalies, which are notoriously hard to detect. Okmok II is built around seven levels of data processing and is interfaced with a new Web-based visualization tool (Figure 5). If triggered, an e-mail alert is sent directly to the ASTER Emergency Scheduling Interface and Control System (AESICS) database to immediately initiate the ASTER scheduling process.

4.2 ASTER Tasking and Collection

In support of the ASTER project, and for use with other applications, the LP DAAC created the ASTER Overpass Predictor to simplify the determination of future ASTER tasking opportunities. The data entry page includes the scene center latitude and longitude, and desired forecast window (Figure 6). Returned results identify possible dates, day or night opportunities, and which ASTER subsystems would be available. In addition to supporting the north Pacific volcano monitoring applications, this tool is now routinely used in support of other emergency response and research activities.

After an anomalous thermal event is detected, AVO initiates an ASTER tasking request and notifies the LP DAAC. These incoming requests are logged in a database included in AESICS. AESICS is a Web-based tool that was created to simplify tasking request submission and to control these requests (Figure 7). New tasking requests can be entered either manually or through the automated procedure, which begins through processes in place at AVO. After new requests are logged in the AESICS database, e-mail notifications are immediately forwarded to the ASTER team at JPL for the actual scheduling using pre-

existing mission protocols. Approvals to task the sensor occur at each stage of the process to ensure the best use of available resources and compliance with mission requirements and international agreements. For example, if there are multiple AVHRR alerts over a particular volcano in a given day, the system of checks guarantees that the ASTER scheduling system is not overloaded.

Following final approvals, and after confirming the absence of scheduling conflicts, the ASTER JPL team accesses the ASTER scheduling system at ERSDAC in Japan and the tasking request is uploaded. The final schedule is determined at ERSDAC and provided to the GSFC Flight Operations Team (FOT) for uplink to the Terra spacecraft. This entire process can be as quick as several hours. Once the data are acquired, they are stored in the Terra solid state recorder until downlink to receivers at White Sands, New Mexico. Raw data are transferred from White Sands via network to GSFC EDOS for initial processing from the raw image data format and then sent to the LP DAAC.

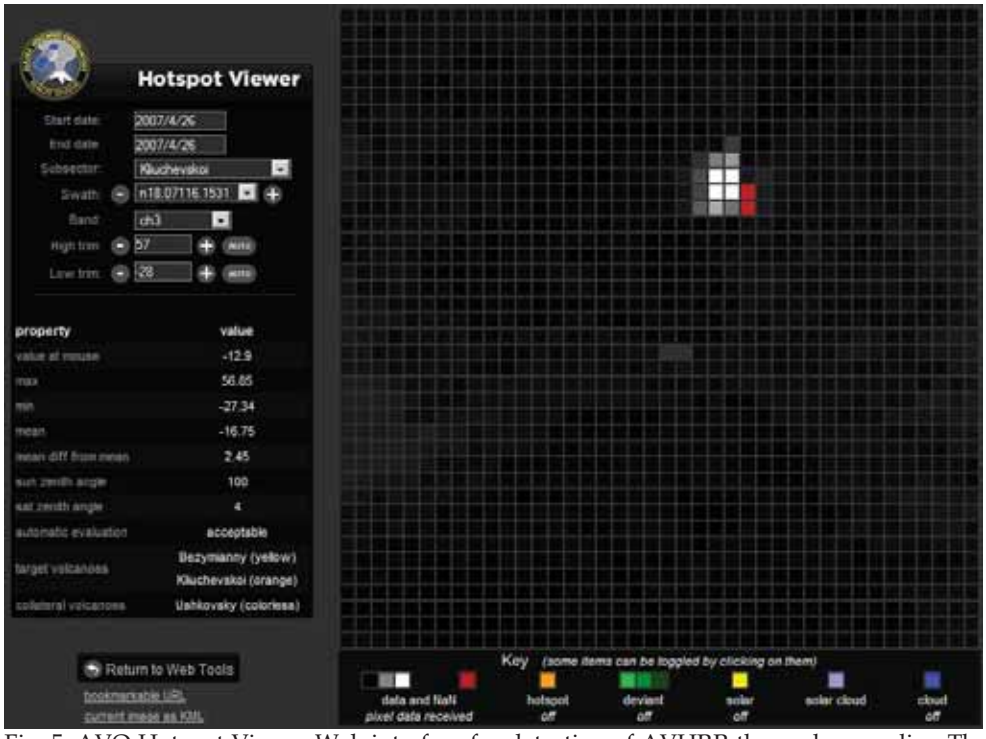

Fig. 5. AVO Hotspot Viewer Web interface for detection of AVHRR thermal anomalies. The AVHRR pixels are reformatted into 1-km grid cells with user-selectable tools for data enhancement. This tool is used to screen for actual anomalies and trigger an ASTER observation. Shown here are the data collected on April 26, 2007 from AVHRR on NOAA-18 for Kliuchevskoi volcano. This data viewer is also used by AVO in their routine volcano monitoring operations. (http://avo-animate.images.alaska.edu/auto_obs_viewer.php)

The ASTER Mission

ASTER is a joint endeavor involving NASA, Japan's Ministry of Economy, Trade and Industry, and other organizations. The ASTER sensor was launched in 1999 on the Terra spacecraft as part of NASA's Earth Observing System with the goal of conducting a global land mapping mission. ASTER has been accomplishing this goal very successfully, having already acquired over 1.5 million scenes. Though the instrument design life has been exceeded, ASTER continues to acquire approximately 450 new 60 by 60 km images of Earth's land surfaces daily, providing Earth land surface information useful for a wide variety of applications.

Terra orbits Earth once every 98.88 minutes at an elevation of 705 km in a sun-synchronous orbit at an inclination of 98.3 degrees. The descending orbit has a 10:30 AM equatorial crossing time and the revisit time is 16 days at the equator (less at higher latitudes or when off-nadir pointing is used). ASTER is tasked through scheduled observations at an 8% duty cycle, and has three imaging subsystems: VNIR, SWIR and TIR. Ground resolution is 15m for VNIR, 30m for SWIR, and 90m for TIR. ASTER has 14 spectral bands ranging from 0.52 micrometers to 11.65 micrometers, including a back-looking VNIR band 3 that enables the generation of digital elevation models. Data are distributed in the HDF-EOS format by the LP DAAC in the USA and by ERSDAC in Japan. More information is contained in Yamaguchi et al. (1998).

Level-1A reconstructed unprocessed instrument data are archived, and other products are generated from these data at the request of customers. Additional products include registered radiance at the sensor, surface reflectance, brightness temperature, surface kinetic temperature, surface emissivity, decorrelation stretch, polar surface and cloud classification, orthorectified, and digital elevation model (Abrams, 2000). The file size of the registered radiance product is approximately 118 MB, and contains data from each subsystem that are geometrically co-registered and radiometrically calibrated.

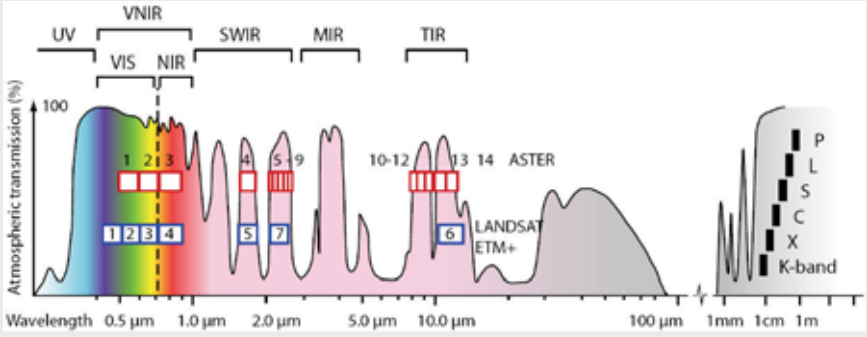

The Earth's atmospheric windows with the spectral coverage of various instruments shown. ASTER (shown in red), Landsat ETM+ (shown in blue), and SAR (shown in black). (Kaab, 2005)

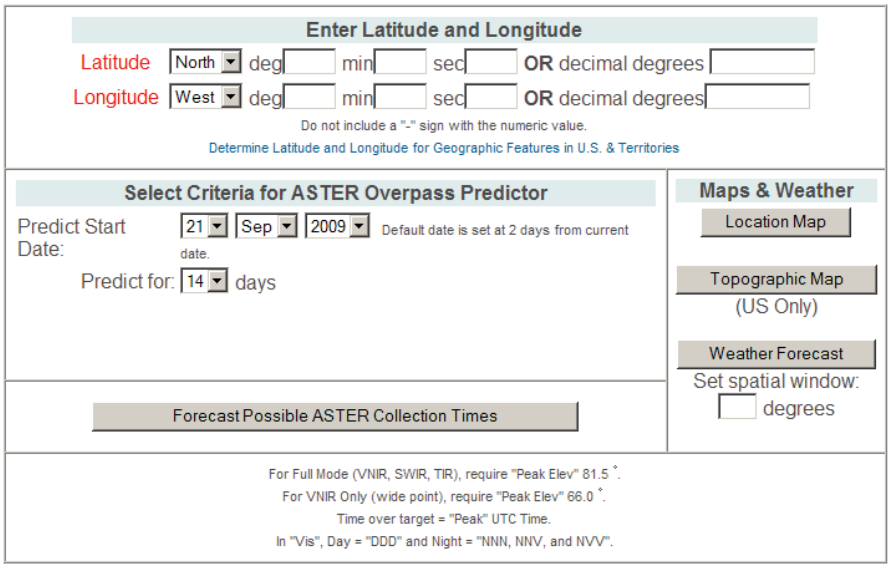

Fig. 6. ASTER Overpass Predictor Web page.
(http://igskmncnwb001.cr.usgs.gov/aster/estimator/reference_info.asp)

4.3 ASTER Data Processing and Distribution

Following standard ASTER mission protocols, raw ASTER data from the Terra spacecraft are processed by EDOS to Level-0. Level-0 data are then transferred via network to LP DAAC. LP DAAC receives the Level-0 data and processes it to Level-1 using executable code and observation schedule information received from ERSDAC. Upon completion of Level-1 processing, data are staged for retrieval via FTP. LP DAAC created a Recent Expedited Production Web site for this project to simplify and speed initial data assessment and downloading of ASTER expedited data. Data are also made available via AESICS, an FTP site, and through the Warehouse Inventory Search Tool (WIST) data search and order mechanism.

Employing the ASTER expedited approach greatly assists in the timely availability of image data for analysis. ASTER expedited data are typically available within six hours after collection, whereas the standard data product availability takes several days after acquisition. This lag time was actually several weeks when the URP volcano monitoring program was first conceived.

ASTER expedited products are very similar to standard products but there are some minor differences. Expedited data do not contain the back-looking band 3, so stereo data are not initially available for digital elevation model (DEM) generation. DEMs can be created later once the standard Level-1 products become available. In addition, short-term calibration for

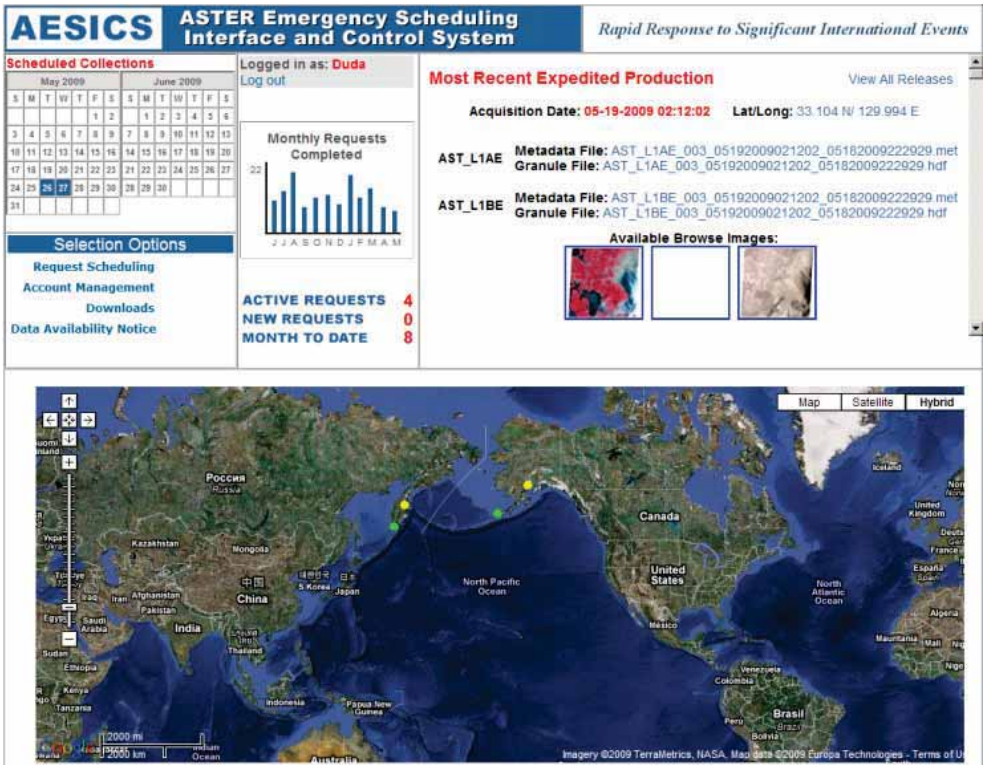

Fig. 7. AESICS Web-based interface. Users can rapidly access statistics on the number of ASTER urgent requests in the last month and year, thumbnail images of the most recent acquisitions, and a map-based display of all ASTER tasking requests in the past 30 days. Based on the Google Earth application, this interface allows users to see which ASTER tasks are new (red dot), approved (yellow dot), and completed (green dot). Each target can also be queried for more information.

the TIR is not available so long-term calibration is used. As a result, expedited TIR data quality is expected to be somewhat reduced. Inter-telescope registration quality is also slightly lower since numerous adjacent scenes are not available as is normally the case. Finally, expedited processing uses raw spacecraft ephemeris data, so the geometry is slightly different than for the data produced using standard processing, which uses refined (post-processed) ephemeris data. Even with these caveats, the image data are still of excellent quality and commonly used to report the latest activity and thermal output values.

4.4 ASTER Data Analysis and Alert Status Updates

After ASTER Level-1 data are processed, image analysts and volcanologists at AVO and the University of Pittsburgh obtain the images for inspection to gain further insight on the current state of the volcano. This may include a visual assessment of the available bands, a characterization of temperature conditions, areal extent of the anomaly, time series analysis,

documentation of flow patterns, and plume extent and content. New data are compared with historical satellite data and other information to identify trends. If warranted, volcano status alerts are updated to notify government authorities and other interested individuals. The volcano monitoring plan is also then updated to ensure that continued observations occur as needed.

5. The 2007 Eruption of Kliuchevskoi Volcano, Russia

One of the most volcanically active regions in the world is Kamchatka, Russia, which is located in the northwestern region of the Pacific Ocean. Several of the more than two dozen active volcanoes on this peninsula are commonly erupting at any given time. These eruptions can produce hazards for the sparse local population living near the volcanoes. But of far more consequence are the eruptions that produce larger ash columns, which are carried by the easterly winds into the routes of approximately 200 aircraft and 20,000 people overflying the region each day (Miller and Casadevall, 2000).

Kliuchevskoi is the highest (> 4800 m) and one of the most active volcanoes in Kamchatka. In the last century, summit eruptions have increased in frequency averaging one every 1–2 years. These eruptions are commonly caused by lava interaction with melting snow/ice and start with increased fumarolic activity within the summit crater. This thermal activity is typically followed by Strombolian explosions, the effusion of blocky lava flows, and the generation of hot avalanches and lahars. Less common are the paroxysmal eruptions, which last occurred in 1994. That eruption included a large convecting column, pyroclastic flows, lahars and lava flows. The largest explosive eruption reached 18 km above sea level and travelled approximately 1,000 km southeast into the north Pacific air traffic routes (Miller et al., 1994).

Ground-based techniques for monitoring the remote volcanoes of Kamchatka include seismic and visual observations. In 2007, there were 33 seismic stations deployed in Kamchatka (Chebrov, 2008). Human observations, reports, and a Web-based video camera system are also used. The Web camera has been installed in the town of Klyuchi 30 km north of Kliuchevskoi. Using the Web-based system, the height of the eruption column has been correlated with the level of seismic activity, thereby allowing seismic signals to predict the height of the eruption plume at night or in times of bad weather (McNutt, 1994; Roach et al., 2004). In addition to these data, high temporal/low spatial resolution orbital remote sensing monitoring of these remote volcanoes has been used for nearly two decades by volcanologists in Russia and the United States. ASTER has been an integral part of this monitoring since it was launched in 1999. Some of the first scientific images collected by ASTER in early 2000 were of the large eruption deposits of Bezymianny volcano (Ramsey and Dehn, 2004). Beginning in 2004, the ASTER rapid response/urgent request system has been linked to the routine remote sensing monitoring done by AVO and KVERT. The ASTER data from this collaborative program have provided the basis for enhanced monitoring efforts, new discoveries, and numerous scientific results (Carter et al., 2007, 2008; Ramsey et al., 2004; Rose and Ramsey, 2009).

During the period between 2000 and 2008, Bezymianny volcano, 10 km south of Kliuchevskoi, was nearly continuously active with approximately two large eruptions per year (Ramsey and Dehn, 2004; Carter et al., 2007). Therefore, this volcano produced numerous AVHRR thermal alerts and subsequent ASTER urgent request images (after the URP system was active). When both Bezymianny and Kliuchevskoi are active, the poor geolocation accuracy of AVHRR makes it difficult to discern which volcano is responsible for producing the thermal anomaly (Dehn et al, 2000). Similarly, both volcanoes commonly appear in one ASTER 60-km scene. It is therefore common for ASTER observations targeting one volcano to capture activity at the other. Typically, low-level thermal activity is seen long before visual or even AVHRR spaceborne observations detect that activity. The better radiometric accuracy, higher spatial resolution, and more precise geolocation of ASTER compared to AVHRR makes the TIR data ideal for detection of the very early stages of new activity at a volcano. However, the poorer temporal frequency commonly limits this important aspect of ASTER. Future TIR instruments with a temporal frequency of hours to days will provide a critically important new dataset for volcano monitoring and eruption prediction.

The detection of renewed activity at Kliuchevskoi first occurred in 2005 in an ASTER TIR scene collected to observe the waning stages of an eruption at Bezymianny (Rose and Ramsey, 2009). A similar situation occurred nearly two years later when observations of the 2006 eruptive activity at Bezymianny also showed a very slight increase in thermal output (~ 5 °C above background) at the summit of Kliuchevskoi as early as November 2, 2006. This activity was noted but did not raise concern due to its very low level and no other detectable activity from visual or seismic observations. On November 27, 2006 the activity remained unchanged. It was not until the first detection by AVHRR on December 14, 2006 that a rapid increase in activity was noted. Two AVHRR pixels between 10 and 30 °C above the average background temperature were detected at the summit, which likely meant that very hot gases and/or small amounts of lava had reached the surface. By December 22, 2006 the activity had further increased enough to trigger an ASTER urgent request image, which was scheduled for January 4-5, 2007 (Figure 8). No activity was detected in the subsequent ASTER VNIR data although a pixel-integrated brightness temperature of 332 °C was extracted from the SWIR data. By January 12, 2007 the color-code for Kliuchevskoi was raised from green to yellow indicating that heightened activity was taking place. However, this activity was low-grade enough that the first ground-based visible observations of a vigorous steam plume and the presence of lava at the summit were not confirmed until February 16, 2007.

Commonly, the winter weather in Kamchatka is clear and cold. Minimal to no cloud cover can be the norm for long stretches between December and May in this region, thereby making optical remote sensing an excellent tool. In the spring and summer months, low-level thicker clouds typically form after 9am and can persist the entire day. These clouds can hinder ground-based visual observations and make visits to the summits of the volcanoes difficult. However, the clouds typically do not extend high enough to obscure the summits of the taller volcanoes such as Kliuchevskoi. For these periods, it is not uncommon that optical remote sensing is the only form of monitoring possible. Higher altitude thin clouds, thin volcanic plumes, and jet contrails can also be problematic for optical remote sensing. These clouds are visually hard to detect, but can negatively-impact the extraction of accurate

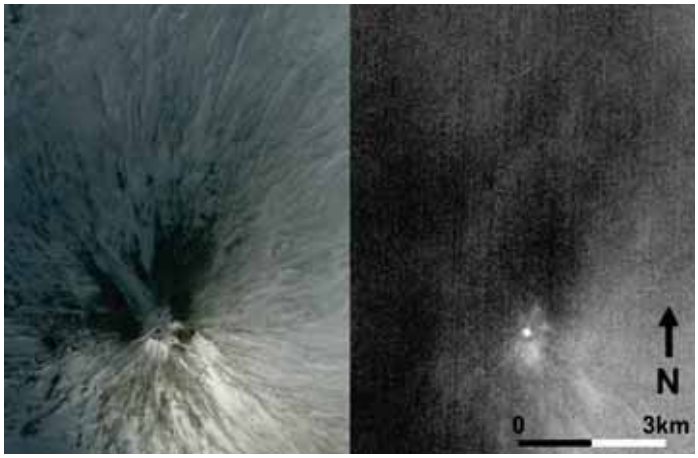

Fig. 8. ASTER data collected on January 4, 2007 and centered on the summit of Kliuchevskoi volcano. The VNIR color composite image (left) shows almost no signs of activity other than a small darker spot in the center of the summit crater (indicating snowmelt) and a minor amount of steam. The band 9 SWIR image (right) however shows a distinct thermal anomaly centered over the dark spot in the summit crater. The maximum integrated brightness temperature derived from the SWIR data was 332 °C indicating the presence of hot gases and/or magma very close to the summit.

surface composition and temperature. For example, this can be seen in the lower surface temperatures derived during periods of thin cloud cover for Kliuchevskoi (Figure 9). From mid-January through mid-April, ASTER continued to collect regularly scheduled and urgent request data of the volcanic activity at Kliuchevskoi. During this period, ground-based observations were hindered at times by the presence of low-level cloud cover. However, these clouds were commonly lower than the summit of Kliuchevskoi allowing the activity to be observed with ASTER and AVHRR. The summit activity continued to increase during this time, producing more thermally elevated pixels and raising the brightness temperature enough to saturate the ASTER SWIR data by early April (Figure 9). This was caused by the presence of a large amount of non-crusted lava in the summit crater from either a small actively overturning lava lake or very vigorous Strombolian eruption activity. On April 9, 2007 the clouds had diminished and photographs from the ground confirmed the Strombolian explosions and the presence of lava that was flowing down the northern slope at a location nearly identical to the 2005 flow (Rose and Ramsey, 2009).

ASTER captured another day/night pair of urgent request images on April 26-27, 2007 (Figure 9). By this time, the active lava flow had been present for over a month and the SWIR and TIR data were commonly saturated in many locations due to the high temperatures. These lava flows were producing numerous lahars that were emplaced 10-15 km further down the northern slope from the base of the lava flow. During this period, larger Vulcanian-style eruptions were also common at the summit crater. These short-duration explosions produced ash columns 5-15 km above the summit, which then commonly drifted S-SE over the peninsula and into the northern Pacific Ocean.

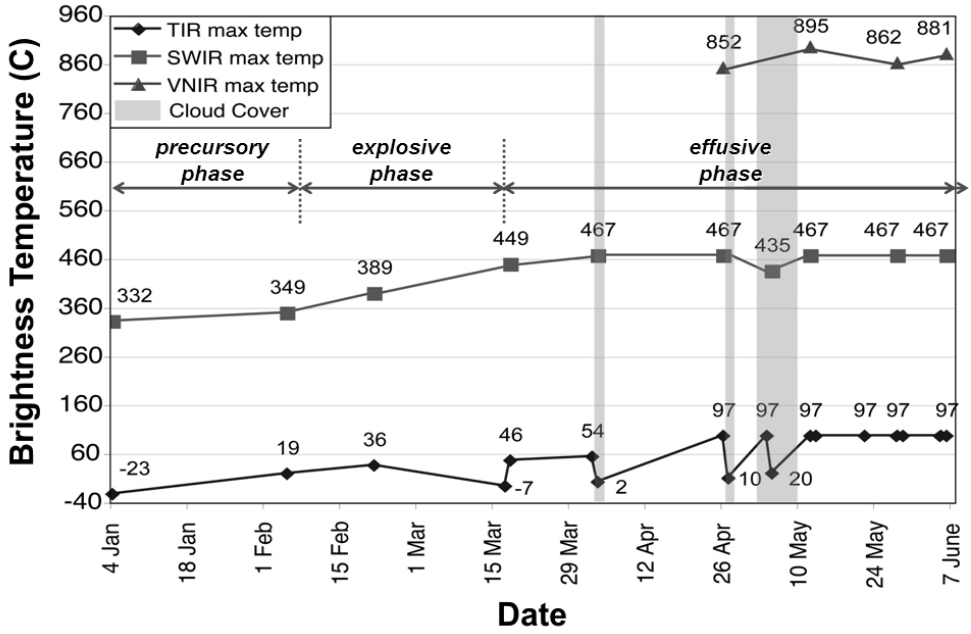

Fig. 9. Time-temperature plot of the 2007 eruption of Kliuchevskoi volcano showing the extracted pixel-integrated brightness temperatures for the three wavelength regions and the three phases of eruptive activity.

The plumes also produced proximal airfall deposits easily seen in contrast to the underlying snow (Figure 10). The April 26-27, 2007 ASTER image pair was unique in several other ways. The data were collected several hours before an AVHRR overpass, which had triggered the next ASTER urgent request (later acquired on May 4-5, 2007). However, because the AVHRR data are displayed on the AVO Web site (see Figure 5) within minutes to hours after collection, this image was seen before the ASTER data and initial descriptions of the activity on April 26 were based on the AVHRR data. The collection of both these datasets within hours of each other provided a rare opportunity to compare detailed ground data/features at the 15- to 90-m scale to what was imaged by the AVHRR instrument at 1-km spatial scale. AVHRR had 23 thermally-elevated pixels, five of which were saturated. The poor spatial resolution did not allow the discrimination of the two lava flows; however, the wide area of hot AVHRR pixels in conjunction with two recovery pixels at the far eastern edge of the thermally elevated area indicated that a new active lava flow was likely present, which was then later confirmed in the ASTER data. Recovery pixels are defined as areas with anomalously low temperatures that commonly occur on the down-scan margin of very high temperature thermal features (Higgins and Harris, 1997). This adverse response of the detectors to a zone of high radiance is produced by a slight delay during which time the previously saturated detector elements equilibrate and no data are collected.

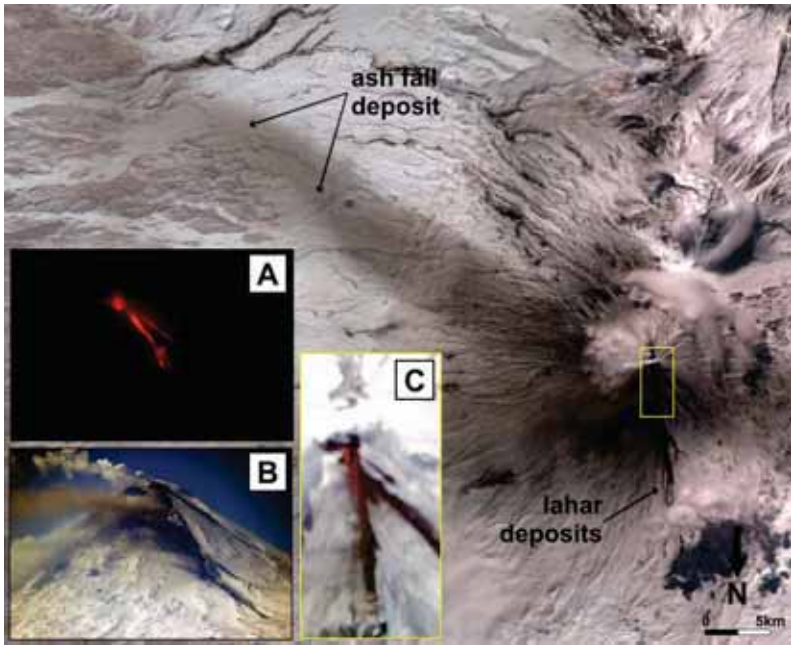

Fig. 10. Kliuchevskoi eruption captured April 24-26, 2007. The base figure, an ASTER VNIR image collected on April 26, 2007, shows a wider area around the volcano and is displayed with North down (opposite to the other ASTER images shown). This allows a similar view as the field photographs **(A and B)** taken from the town of Klyuchi by Y. Demyanchuk. In the ASTER image, an ash fall deposit to the SE, numerous lahar deposits to the N, and a vigorous steam plume at the summit are all visible. **(A)** Nighttime photograph of the summit taken on April 24, 2007 showing the Strombolian activity and two distinct lava flows. **(B)** Daytime photograph taken one day later (and one day before the ASTER image) showing both lava flows and the dendritic patterns of the lahar deposits all of which are clearly visible in the ASTER image. **(C)** Enhanced linear stretch of the ASTER VNIR data of the summit region (denoted by the yellow rectangle). The active incandescent lava flows are seen and the maximum brightness temperature extract from these data was 852 °C.

A cold plume extending to the NE in the AVHRR image (and not seen in the ASTER image) indicated the volcano was continuing to produce larger eruptions every few hours during the lava flow emplacement phase. These plumes were carried in different directions (SE in ASTER, NE in AVHRR) depending on the local wind at the time. Once the ASTER data were available, it was confirmed that lava was now being emplaced in a new direction and that the previous lava flow was beginning to cool. This new lava flow was active and large enough to be seen in the 15m VNIR data (Figure 10C). At that point the open channel was 15-30 m wide, 3 km long and had a pixel-integrated brightness temperature of 852 °C. To extract brightness temperatures in daytime VNIR or SWIR data, the solar reflected contribution in each pixel had to be removed. This was done by calculating that amount in each wavelength band using non-thermally-elevated pixels from a nearby region under similar lighting conditions (Rose and Ramsey, 2009). The flow was being emplaced to the

north, in the large volcano shadow because of the low sun angle at this latitude and this time of year. Therefore, the solar correction was minimal and the extracted brightness temperatures from the VNIR and SWIR data were much more accurate.

This dataset also marked the start of approximately two months of nearly cloud-free ASTER data where the locations of the lava flows and their VNIR-derived temperatures were tracked and used for detailed monitoring of the eruption (Figures 9-11). The extracted pixel-integrated brightness temperatures were divided into three phases of activity, which also correlated with visible observations and seismic data. In the precursory phase (November 2006 to February 2007), TIR temperatures began to rise above the average background temperature (approximately -40 °C in January) and became hot enough to be detected by the SWIR data. This phase was dominated by fumarolic degassing and minor Strombolian activity at the summit. In the explosive phase (February 2007 to March 2007), degassing became more intense and Strombolian explosions at the summit were nearly constant. However, the amount of lava was not large enough to saturate either the TIR or SWIR data. Beginning in mid-March 2007 and continuing until mid-June 2007, the effusive phase was ongoing with the emplacement of three large basaltic andesite lava flows. Each of these flows contained an active center channel for long periods of time resulting in the saturation of both the TIR and SWIR data and allowing temperatures to be extracted from the 15-m VNIR data. These pixel-integrated temperatures are slightly lower than similarly derived temperatures for Hawaiian lava flows indicating that the actual temperature of the lavas were between 1050 and 1100 °C (Ramsey and Wessels, 2007).

From mid-April to mid-June, Kliuchevskoi produced three new lava flows, small-scale Strombolian summit activity, and larger explosive eruptions resulting in ash plumes that extended to the east hundreds of kilometers. On May 29, 2007 the nighttime ASTER TIR image clearly showed the three N-NW lava flows and a weak TIR signal extending approximately 400 m to the SE of the summit crater. This linear thermal anomaly was predicted to be the start of new lava flow direction but was not confirmed until the next ASTER image pair on June 6-7, 2007 (Figure 11). The prediction of this new flow direction was initially discounted by most observers/scientists because of the high level of activity ongoing to the north and lack of historical lava flows emanating from the summit in this direction. The data collected on June 6, 2007, verified that the northern lava flows were no longer active. Their temperatures (between 10-20 °C above the background temperature) had cooled well below the detection threshold for ASTER VNIR and SWIR but could still be discerned in the TIR image. The most obvious change was the presence of two new SE trending active lava flows in the exact direction as the linear thermal anomaly seen in the May 20, 2007, image. The larger flow was 3.1 km long and was emplaced at an average rate of 16 m/hr, which was nearly the same flow rate as the northern flows. However, the flow rate increased significantly near the end of the effusive phase of the 2007 eruption. The flow rate was calculated by examining changes in the small flow south of the larger SE flow (Figure 11B). ASTER collected a nighttime image 13 hours after the data shown in Figure 11 and the advancement of this flow was easily seen. Using the digital elevation model derived from the VNIR image (Figure 11A), the slope in this region was calculated and used to derive a flow rate of 26 m/hr. This flow rate continued for the rest of June, after which the

effusive phase ended. The lava flows continued to cool over the next several months and no new explosive activity was observed. The eruption was officially declared over in July 2007.

During the six month long 2007 eruption of Kliuchevskoi, ASTER provided unprecedented views of the summit activity. The eruption began in the winter, making ground or helicopter observations nearly impossible because of the harsh conditions. As the weather warmed, cloud cover further limited ground views of the summit. Thirty-two ASTER images were acquired during the day and night over this time period, which was an average of one scene every six days, although many images were day/night pairs collected 13 hours apart. Of this total, three day/night pairs (January 4-5, March 17-18, May 4-5) were collected as a result of the automatic triggering of the ASTER urgent request system. An additional seven image pairs were also acquired using the manual tasking of this urgent request system. The manual tasking was used during cloudy periods where AVHRR data were limited or to augment the volume of automatically tasked images. The ASTER URP program therefore produced a 63% increase in the data volume during the eruption of Kliuchevskoi, making it an invaluable tool for monitoring. The twelve additional ASTER images collected during this time period were part of the routine volcano monitoring performed by ASTER for all active volcanoes around the world (Pieri and Abrams, 2004).

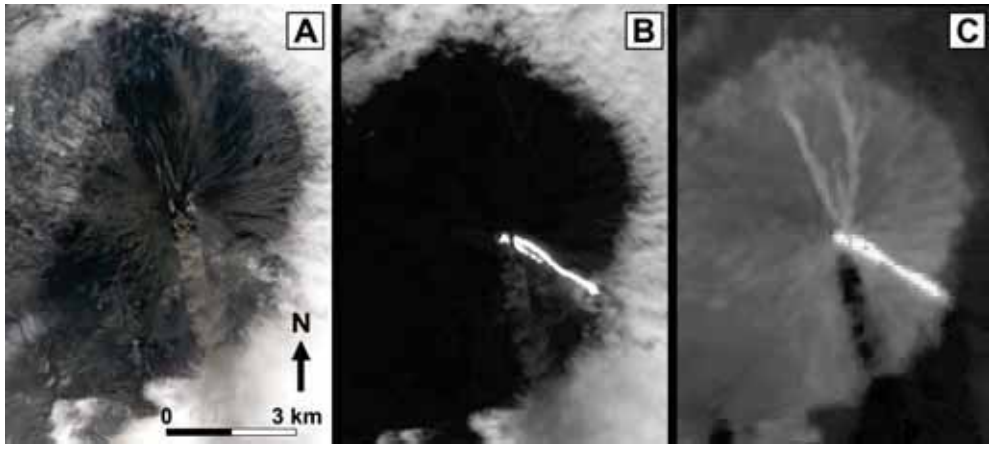

Fig. 11. ASTER urgent request data collected on June 6, 2007 over the summit region of Kliuchevskoi volcano. **(A)** VNIR image now showing the lack of snow on the upper flanks of the volcano and an ash-rich plume from the summit crater and extending southward. Note the low level cloud deck surrounding the volcano at ~2500 m. Such clouds are common starting in the spring and completely obscure ground observations. ASTER provided the only detailed record of eruptive activity during this period. **(B)** SWIR band 4 image covering the same area. The summit crater and SE trending lava flow are clearly visible, as is a secondary breakout flow to the south of the larger flow. Using the ASTER-derived DEM of the summit and the difference in the flow lengths between the day and nighttime images (ΔT = 13 hours), the flow velocity was calculated to be 26 m/hour. This was significantly faster than the previous lava flows to the N and NW. **(C)** TIR band 10 image showing the active lava flow, the colder plume, and the two previous lava flows (N and NW) that were still cooling but no longer visible in the VNIR or SWIR data.

The numerous datasets provided by ASTER as part of the collaborative rapid-response program in conjunction with the relatively clear weather and the summit elevation and high latitude of Kliuchevskoi resulted in the largest and most comprehensive multispectral/multispatial high resolution dataset of a volcanic eruption. These data provide another means to monitor and characterize eruptive activity of this region of the globe. Precursors of eruption onset and new behavior can be better recognized using high resolution image data across the wavelength region and thus minimize future risks.

6. Conclusions

The value of using remote sensing assets in geoscience applications has been demonstrated by many authors and detailed here for the north Pacific volcano monitoring program. Numerous successes have been realized using this programmatic approach for capturing higher temporal frequency data, and a more rapid dissemination of critical information has been established for integration with future higher resolution datasets. The work described enabled the incorporation of higher spatial resolution ASTER data into an existing coarser resolution volcano monitoring initiative. New techniques were developed for event detection, satellite tasking, data distribution, and data analysis. These resulted in more rapid data availability, more detailed information, greater scientific insight on geologic processes, and more reliable alerts to the communities involved.

Specifically for Kamchatka, several beneficial factors have combined resulting in nearly 1,400 ASTER images of the five most thermally active Kamchatka volcanoes (Bezymianny, Karimsky, Kliuchevskoi, Sheveluch and Tolbachik). These factors include the orbital alignment of Terra, the high latitude of the peninsula, and the persistent activity in this region. From the inception of the automated rapid response program in 2004, an additional 350 scenes have been acquired over these volcanoes, many soon after larger eruptions. These data have produced valuable quantitative information on the small-scale activity and larger eruptions. A detailed example of the 2007 eruption of Kliuchevskoi described here enabled fundamental lava flow parameters to be determined. Numerous eruptions have been observed in Kamchatka by ASTER, which have displayed varying volcanic styles including basaltic lava flow emplacement, silicic lava dome growth, pyroclastic flow emplacement, volcanic ash plume production, fumarolic activity, and geothermal emission. The high spatial resolution and moderate spectral resolution of the data are ideal for deriving the energy flux from both high and low temperature systems, mapping chemical and textural changes of the volcanic products, and for imaging and understanding recent volcanic deposits.

The international collaboration developed for this work created professional relationships and infrastructure that will prove valuable in future work. The focus of further research will be on specific eruptions of the Kamchatka and Alaska volcanoes, the science results stemming from those data, expansion plans for global ASTER urgent request data and support for other types of events. The current ASTER rapid response program in Kamchatka and Alaska has produced a large archive of data, which has only been sampled to a small degree. These data offer a source for both the timely completion of current studies and new scientific analysis. It has also improved the timeliness and reliability of resulting hazard

notifications to responsible authorities and affected communities. However, it should be noted that the ASTER instrument has long exceeded its initial design life. The SWIR subsystem has now failed and the sensor could suffer further catastrophic losses at any time. Therefore, there is a critical need for a continuing series of sensors with similar characteristics to ASTER in order to support such geoscience applications.

7. Acknowledgements

The URP project described here was made possible by the efforts and support of the ASTER Science Team and through NASA funding to M. Ramsey (grants: NNG04GO69G and NNX08AJ91G).The authors would like to thank S. Rose for her detailed research on the Kliuchevskoi ASTER data and helping to create Figure 9. The authors greatly appreciate technical review comments received from Zhong Lu and Russell Rykhus, and editorial assistance from Tom Adamson and Aleksandar Lazinica. ASTER data are courtesy of NASA, GSFC, Japan's Ministry of Economy and Industry, ERSDAC, Japan Resources Observation System and Space Utilization Organization (JAROS), the U.S./Japan ASTER Science Team, and LP DAAC at the USGS EROS Center.

8. References

Abrams, M. (2000). The Advanced Spaceborne Thermal Emission and Reflectance Radiometer (ASTER): data products for the high spatial resolution imager on NASA's Terra platform. *International Journal of Remote Sensing*, 21, 847−859.

Carter, A.J., Ramsey, M.S., and Belousov, A.B. (2007). Recent crater formation at Bezymianny Volcano lava dome: Significant changes observed in satellite and field data, *Bull. Volc.*, doi: 10.1007/s00445-007-0113-x..

Carter, A.J., Girina, O., Ramsey, M.S., and Demyanchuk, Y.V. (2008). ASTER and field observations of the 24 December 2006 eruption of Bezymianny Volcano, Russia, *Rem. Sens. Environ.*, 112, 2569–2577, doi: 10.1016/j.rse.2007.12.001.

Chebrov, V. (2008). Complex seismological and geophysical investigation of Kamchatka and Commander Islands. *Annual report of KB GS RAS*. Ed. V. Chebrov. pp. 268. (in Russian).

Dean, K., Servilla, M., Roach, A., Foster, B., and Engle, K. (1998). Satellite monitoring of remote volcanoes improves study efforts in Alaska, EOS, *Trans. Amer. Geophys. Union*, 79, 413, 422-423.

Dehn, J., Dean, K.G., and Engle, K. (2000). Thermal monitoring of north Pacific volcanoes from space, *Geology*, 28, 755-758.

Dehn, J., Harris, A.J.L. (in press). Thermal Anomalies at Volcanoes. in: *Monitoring Volcanoes in the North Pacific: Observations from Space*, Dean K.G. and Dehn J. editors, Praxis/Springer.

Fournier, T., J. Freymueller, and P. Cervelli (2009). Tracking magma volume recovery at Okmok volcano using GPS and an unscented Kalman filter, *J. Geophys. Res.*, 114, B02405, doi:10.1029/2008JB005837.

Harris, A.J.L., Flynn, L.P., Keszthelyi, L., Mouginis-Mark, P.J., Rowland, S.K., and Resing, J.A. (1998). Calculation of lava effusion rates from Landsat TM data, *Bull. Volc.*, 60, 52-71.

Higgins, J. and Harris, A. (1997). VAST: A program to locate and analyse volcanic thermal anomalies automatically from remotely sensed data, *Computers & Geosci*., v. 23. n. 6, pp. 621-645.

Kaab, A. (2005). *Remote sensing of mountain glaciers and permafrost creep*, Physical Geography Series, Zurich, 48, 266 pages, ISBN 3 85543 244 9.

Lu, Z., D. Dzurisin, C. Wicks, J. Power, O. Kwoun, and R. Rykhus (2007). Diverse deformation patterns of Aleutian volcanoes from satellite interferometric synthetic aperture radar (InSAR), in *Volcanism and Subduction: The Kamchatka Region* (edited by J. Eichelberger et al.), American Geophysical Union Geophysical Monograph Series 172, 249-261.

McNutt, S.R. (1994). Volcanic tremor amplitude correlated with the Volcanic Explosivity Index and its potential use in determining ash hazards to aviation. *Acta Vulcanol*. 5. pp193-196.

Miller, T.P., Kirianov, V.Y., Kelley, H.L. (1994). Klyuchevskoy Fact Sheet. *U.S. Geological Survey Fact Sheet. 94-067*, pp. 4. Also online (http://eq.giseis.alaska.edu/volcanoes/klyu/klyufact.html).

Miller, T.P., and Casadevall, T.J. (2000). Volcanic Ash Hazards to Aviation. In: Sigurdsson, H., Houghton, B., McNutt, S.R., Rymer, H. and Stix, J., Editors, 2000. *Encyclopedia of Volcanoes*, Academic Press, San Diego, CA, pp. 915–930.

Pieri, D.C., and Abrams, M.J. (2004). ASTER watches the world's volcanoes: a new paradigm for volcanological observations from orbit. *Journal of Volcanology and Geothermal Research*. 135: 13–28.

Ramsey, M.S. and Dehn, J. (2004). Spaceborne observations of the 2000 Bezymianny, Kamchatka eruption: The integration of high-resolution ASTER data into near real-time monitoring using AVHRR, *J. Volc. Geotherm. Res*., 135, issue 1-2, 127-146.

Ramsey, M.S., Dehn, J., Wessels, R., Byrnes, J., Duda, K., Maldonado, L., and Dwyer, J. (2004). The ASTER emergency scheduling system: A new project linking near-real-time satellite monitoring of disasters to the acquisition of high-resolution remote sensing data, *Eos Trans. AGU*, 85(47), Fall Meet. Suppl., Abstract SF23A-0026.

Ramsey, M.S., and Wessels, R.L. (2007). Monitoring changing eruption styles of Kilauea Volcano over the summer of 2007 with spaceborne infrared data, *Eos Trans. AGU*, 88(52): Fall Meet. Suppl., Abstract V51H-07.

Ramsey, M.S., Anderson, S., and Wessels, R. (2008). Active dome and pyroclastic flow deposits of Sheveluch Volcano, Kamchatka: Unique thermal infrared and morphologic field observations, *IAVCEI, General Assem. Prog*., p. 67.

Roach, A.L., Benoit, J.P., Dean, K.G., McNutt, S.R. (2004). The combined use of satellite and seismic monitoring during the 1996 eruption of Pavlof volcano, *Alaska. Bulletin of Volcanology*. 62 (6-7): 385-399.

Rose, S.R. and Ramsey, M.S. (2009). The 2005 eruption of Kliuchevskoi volcano: Chronology and processes derived from ASTER spaceborne and field-based data, *J. Volc. Geotherm. Res*., doi:10.1016/j.jvolgeores.2009.05.001.

Schneider, D., Dean, K.G., Dehn, J., Miller, T.P., and Kirianov, V. Yu. (2000). Monitoring and analyses of volcanic activity using remote sensing at the Alaska Volcano Observatory: case study for Kamchatka, Russia, December 1997. *Remote Sensing of Active Volcanism*, Geophysical Monograph 116, 65-85.

Stephens, C. D., and Chouet, B. A. (2001). Evolution of the December 14, 1989 precursory long-period event swarm at Redoubt Volcano, Alaska*: Journal of Volcanology and Geothermal Research*, v. 109, n. 1, p. 133-148.

Wessels, R.L., Schneider, D.J., Coombs, M.L., Dehn, J., and Ramsey, M.S. (in press). High-resolution Satellite and Airborne Thermal Infrared Imaging of the 2006 Eruption of Augustine Volcano, Alaska**,** *in* Power, J.A., Coombs, M.L., and Freymueller, J.T., eds., *Investigations of Augustine Volcano, Alaska after the 2006 eruption*, U.S. Geological Survey, Professional Paper.

Wright, R., Flynn, L., Garbeil, H., Harris, A., and Pilger, E. (2002). Automated volcanic eruption detection using MODIS, *Rem. Sens. Environ*., 82, 135-155.

Yamaguchi, Y., Kahle, A. B., Tsu, H., Kawakami, T., & Pniel, M. (1998). Overview of Advanced Spaceborne Thermal Emission and Reflection Radiometer (ASTER). *IEEE Transactions on Geoscience and Remote Sensing*, 36, 1062−1071.

Yang, F. and Schlesinger, M.E. (2002). On the surface and atmospheric temperature changes following the 1991 Pinatubo volcanic eruption; a GCM study, *J. Geophys. Research*, 107; 7-8.